Inorg. Chem. **2006**, *45*, 8452–8458

Organically Directed Iron Sulfate Chains: Structural Diversity Based on Hydrogen Bonding Interactions

Yunlong Fu,* Zhiwei Xu, Jialin Ren, Haishun Wu, and Rong Yuan

School of Chemistry and Material Science, Shanxi Normal University, Linfen Shanxi, China 041004

Received June 13, 2006

Six organically directed 1-D iron sulfates hydrated and hydrolyzed to different extents have been prepared hydrothermally. $[C_2H_{10}N_2]_{1.5}[Fe(SO_4)_3]\cdot 2H_2O$ (**I**), $[C_2H_{10}N_2][Fe(SO_4)_2(OH)]\cdot H_2O$ (**II**), $[C_6H_{18}N_2]_{0.5}[Fe(SO_4)_2(H_2O)_2]$ (**III**), and $[C_6H_{18}N_2]_{0.5}[Fe_2(SO_4)(H_2O)_4(OH)]\cdot H_2O$ (**V**) possess the linear topological structures observed in ferrinatrite, sideronatrite, kröhnkite, and copiapite minerals, respectively. $[C_4H_{12}N_2][Fe_2(SO_4)_3(OH)_2(H_2O)_2]\cdot H_2O$ (**IV**) shows a novel linear structure that can be regarded as a hybrid of the tancoite and butlerite types. $[C_6N_4H_{22}]_{0.5}[Fe(SO_4)_2(OH)]\cdot 2H_2O$ (**VI**) adopts a cis configuration, compared with **II**, to give a rare inorganic helical iron sulfate chain which is a new member of the organically directed transitional metal sulfates. The results reveal that the starting molar proportion of the reactants and the type of amines are critical for the structural motif. There is an obvious relationship between the constitution of chains and the type of amino groups, involving the amount of N–H···O hydrogen bonds.

Introduction

The aqueous chemistry of transition metal ions, especially the Fe^{3+} ion, is complex and charming, partly because of their interesting hydrolyzation and polymerization behaviors.[1] The isolation and structural characterization of hydrolyzed and polymerized components are also of importance for metal aqueous chemistry and the synthesis of novel materials.

Organic amines as structural directing agents (SDA's) have shown outstanding effects in directing the inorganic open frameworks, such as phosphates,[2] arsenates,[3] germinates,[4] and selenites.[5] On the basis of the static charge interactions, hydrogen-bonding interactions, filling effects, etc.,[6] their influences are mainly embodied in aspects such as control of the dimension and the pore size of the inorganic open framework, and they further result in various physical and chemistry properties. Incorporation of the appropriate amine may provide an effective route for the isolation and modulation of such oxo-metal clusters and relative inorganic frameworks. For example, a sulfate group was introduced as an anionic moiety of the framework. Organically directed metal sulfate chemistry is at a somewhat nascent stage. Rao et al. synthesized the first members of cadmium sulfate families by adopting an amine−sulfate route.[7] By employing fluoride, they have reported a series of organically directed metal sulfates, such as iron,[8] nickel,[9] and cobalt[10] sulfates. However, the transition metal sulfate system without fluoride is relatively undeveloped, and only a few compounds have

* To whom correspondence should be addressed. Phone: +86 357 2053716. Fax: +86 357 2053716. E-mail: yunlongfu@dns.sxnu.edu.cn.

(1) (a) Spiro, T. G.; Allerton, S. E.; Renner, J.; Terzis, A.; Bils, R.; Saltmanlb, P. *J. Am. Chem. Soc.* **1966**, *88*, 2721. (b) Richmond, W. R.; Hockridge, J. G.; Loan, M.; Parkinson, G. M. *Chem. Mater.* **2004**, *16*, 3203. (c) Cai, J.; Liu, J.; Gao, Z.; Navrotsky, A.; Suib, S. L. *Chem. Mater.* **2001**, *13*, 4595. (d) Jolivet, J. P.; Chanéac, C.; Tronc, E. *Chem. Commun.* **2004**, 481.

(2) Cheetham, A. K.; Férey, G.; Loiseau, T. *Angew. Chem., Int. Ed.* **1999**, *38*, 3268−3292.

(3) (a) Locock, A. J.; Burns, P. C. *J. Solid State Chem.* **2003**, *176*, 18. (b) Bortun, A. I.; Bortun, L. N.; Espina, A.; Garciab, J. R.; Clearfield, A. *J. Mater. Chem.* **1997**, *7*, 2525. (c) Bazan, B.; Mesa, J. L.; Pizarro, J. L.; Aguayo, T. A.; Arriortua, M. I.; Rojo, T. *Chem. Commun.* **2003**, 622. (d) Ekambaram, S.; Sevov, S. *Inorg. Chem.* **2000**, *39*, 2405. (e) Haushalter, R. C.; Wang, Z. W.; Meyer, L. M.; Dhingra, S. S.; Thompson, M. E.; Zubieta, J. *Chem. Mater.* **1994**, *6*, 1463.

(4) (a)Francis, R. J.; Jacobson, A. J. *Chem. Mater.* **2001**, *13*, 4676. (b) Fernandez, S.; Mesa, J. L.; Pizarro, J. L.; Lezama, L.; Arriortua, M. I.; Olazcuaga, R.; Rojo, T. *Chem. Mater.* **2000**, *12*, 2092. (c) Rodgers, J. A.; Harrison, W. T. A. *Chem. Commun.* **2000**, 2385.

(5) (a) Choudhury, A.; Udayakumar, D.; Rao, C. N. R. *Angew. Chem., Int. Ed.* **2002**, *41*, 158. (b) Harrison, W. T. A.; Philips, M. L. F.; Stanchfield, J.; Nenoff, T. M. *Angew. Chem., Int. Ed.* **2002**, *39*, 3808. (c) Udayakumar, D.; Rao, C. N. R. *J. Mater. Chem.* **2003**, *13*, 1635. (d) Pasha, I.; Choudhury, A.; Rao, C. N. R. *J. Solid State Chem.* **2003**, *174*, 386.

(6) Behera, J. N.; Paul, G.; Choudhury, A.; Rao, C. N. R. *Chem. Commun.* **2004**, 456.

(7) (a)Paul, G.; Choudhury, A.; Rao, C. N. R. *J. Chem. Soc., Dalton Trans.* **2002**, 3859. (b) Choudhury, A.; Krishnamoorthy, J.; Rao, C. N. R. *Chem. Commun.* **2001**, 2610.

10.1021/ic061059v CCC: $33.50
Published on Web 09/01/2006

Table 1. Synthetic Conditions for Compounds **I**−**VI**

	starting composition	*T* (K)	time (day)	pH[d]	formula	yield (%)
I	$Fe_2(SO_4)_3$·$9H_2O$/en[a]/H_2SO_4/H_2O/ethanol (1:5:5:278:87)	383	2	2 (2)	$[C_2N_2H_{10}]_{1.5}[Fe(SO_4)_3]\cdot 2H_2O$	60
II	$Fe_2(SO_4)_3$·$9H_2O$/en[a]/H_2SO_4/H_2O/ethanol (1:1:1:278:87)	383	2	2 (2)	$[C_2N_2H_{10}][Fe(SO_4)_2(OH)]\cdot H_2O$	70
III	$Fe_2(SO_4)_3$·$9H_2O$/TMED[b]/H_2SO_4/H_2O/ethanol (1:1:2.2:278:87)	383	2	2 (2)	$[C_6N_2H_{18}]_{0.5}[Fe(SO_4)_2(H_2O)_2]$	30
IV	$Fe_2(SO_4)_3$·$9H_2O$/piperazine/H_2SO_4/H_2O/ethanol (2:1:1:333:130)	383	2	2 (2)	$[C_4N_2H_{12}][Fe_2(SO_4)_3(OH)_2(H_2O)_2]\cdot H_2O$	50
V	$Fe_2(SO_4)_3$·$9H_2O$/TMED[b]/H_2SO_4/H_2O/ethanol (1:1:2.2:278:87)	383	2	2 (2)	$[C_6N_2H_{18}]_{0.5}[Fe_2(SO_4)(H_2O)_4(OH)]\cdot H_2O$	30
VI	$Fe_2(SO_4)_3$·$9H_2O$/TETA[c]/H_2SO_4/H_2O/ethanol (1:0.5:2:333:55)	383	2	2 (2)	$[C_6N_4H_{22}]_{0.5}[Fe(SO_4)_2(OH)]\cdot H_2O$	30

[a] Ethylenediamine. [b] *N*,*N*,*N*′,*N*′-Tetramethylethylenediamine. [c] Triethylenetetramine. [d] The value in the parentheses indicates the final pH.

been reported,[11] although organically directed rare earth metal sulfates have been reported recently.[12]

This article reports six 1-D organically directed iron sulfates synthesized under mild hydrothermal conditions. From the results, the iron sulfates show strong tendencies to form 1-D chains which are sensitive to the given reaction conditions. These compounds are among the few members of the organically directed iron sulfates. This study may provide some valuable information for the rational design and synthesis of transition metal sulfates with different topologies and further elucidation of the structural directing effects of the amines.

Experimental Section

Synthesis and Initial Characterization. All six compounds were prepared under mild hydrothermal conditions. For **I**, 0.285 g of $Fe_2(SO_4)_3$·$9H_2O$ was dissolved in an ethanol/H_2O mixture (5.0 mL/5.0 mL) with constant stirring. To this solution, 0.24 mL of H_2SO_4 (98%) and 0.16 mL of ethylenediamine (en) were added. After it was stirred for 30 min, the final mixture with the molar composition of $Fe_2(SO_4)_3$/en/H_2SO_4/H_2O/ethanol (1:4.5:8:278:287) was transferred into a 15 mL Teflon-lined autoclave and heated at 383 K for 2 days. The colorless rod-shaped crystals were harvested as the major products (60% yield). The pH did not change before or after the reaction. The preparation methods for **II**−**VI** were similar to that of **I**, and the piperazine, *N*,*N*,*N*′,*N*′-tetramethylethylenediamine (TMED), and triethylenetetramine (TETA) were introduced as templates, respectively. Details for the preparation of iron sulfates are listed in Table 1. The initial characterization of **I**−**VI** was carried out using powder X-ray diffraction (P-XRD), thermal gravimetric analysis (TGA), elemental CHN analysis, and IR spectroscopy.

The powder X-ray diffraction patterns of the compounds are in good agreement with the simulated patterns generated from the single-crystal XRD data. The difference in the reflection intensity is probably caused by the preferred orientation effects of the powder sample. In addition, some products are multiphase; for example, **III** and **V** were separated in the same autoclave, and the same situation also occurred in the case of **IV** and another compound, $(C_4H_{12}N_2)[Fe(SO_4)_2OH]$.[13a]

All six compounds were given satisfactory elemental analysis performed on a PE2400CHN element analyzer. The experimental and calculated (in wt %) values for C, H, and N are as follows: **I** C 7.62, N 8.78, H 4.06 (calcd C 7.61, N 8.88, H 4.05); **II** C 6.97, N 8.18, H 3.74 (calcd C 6.96, N 8.12, H 3.80); **III** C 10.60, N 4.04, H 3.01 (calcd C 10.58, N 4.11, H 3.11); **IV** C 8.41, N 4.83, H 3.53 (calcd C 8.33, N 4.85, H 3.67); **V** C 6.39, N 2.48, H 3.54 (calcd C 6.37, N 2.47, H 3.56); **VI** C 10.06, N 7.94, H 3.93 (calcd C 10.06, N 7.82, H 3.94).

The infrared (IR) spectra were recorded within the 400−4000 cm^{-1} region on a Nicolet 5DX spectrometer using KBr pellets. The various multiple bands in the 980−1010 cm^{-1} region are from ν_1, and those in the 1090−1140 cm^{-1} region are from ν_3 of the sulfate groups.[14] The bending modes of sulfate groups are found in the 500−700 cm^{-1} regions. The broad bands are from ν(O−H) and ν(N−H) in the 3000−3500 cm^{-1} region.

The thermal gravimetric analysis (TGA) was performed on a ZRP-2P thermal analyzer. Compounds **III**, **IV**, and **V** were separated manually for TGA. Samples were loaded into a platinum crucible and heated in a nitrogen atmosphere at a heating rate of 10°/min. The TGA curve for each compound shows distinct two-step weight losses corresponding to the loss of the water in the range of 100−230 °C and to the loss of amine and SO_3 in the range of 200−530 °C. The residue after calcination of the products at 660 °C is α-Fe_2O_3 (Inorganic Crystal Structure Database, ICSD, 15840) as proved by powder X-ray diffraction (seen in Supporting Information).

Single-Crystal Structure Determination. Suitable single crystals of all six compounds were manually selected under a polarizing

(8) (a) Paul, G.; Choudhury, A.; Rao, C. N. R. *Chem. Mater.* **2003**, *15*, 1174. (b) Rao, C. N. R.; Sampathkumaran, E. V.; Nagarajan, S.; Paul, G.; Behera, J. N.; Choudhury, A. *Chem. Mater.* **2004**, *16*, 1441. (c) Paul, G.; Choudhury, A.; Rao, C. N. R. *Chem. Commun.* **2002**, 1904.

(9) Behera, J. N.; Gopalkrishnan, K. V.; Rao, C. N. R. *Inorg. Chem.* **2004**, *43*, 2636.

(10) (a) Behera, J. N.; Paul, G.; Choudhury, A.; Rao, C. N. R. *Chem. Commun.* **2004**, 456. (b) Rujiwatra A.; Kepert, C. J.; Rosseinsky, M. J. *Chem. Commun.* **1999**, 2307.

(11) (a) Paul, G.; Choudhury, A.; Nagarajan, S.; Rao, C. N. R. *Inorg. Chem.* **2003**, *42*, 2004. (b) Gutnick, J. R.; Muller, E. A.; Sarjeant, A. N.; Norquist, A. J. *Inorg. Chem.* **2004**, *43*, 6528. (c) Muller, E. A.; Cannon, R. J.; Sarjeant, A. N.; Ok, K. M.; Halasyamani, P. S.; Norquist, A. J. *Cryst. Growth Des.* **2005**, *5*, 1913.

(12) (a) Xing Y.; Liu, Y. L.; Shi, Z.; Meng, H.; Pang, W. Q. *J. Solid State Chem.* **2003**, *174*, 381. (b) Xing, Y.; Shi, Z.; Li, G. H.; Pang, W. Q. *Dalton Trans.* **2003**, 940. (c) Bataille, T.; Louër, D. *J. Mater. Chem.* **2002**, *12*, 3487. (d) Liu, L.; Meng, H.; Li, G. H.; Cui, Y. J.; Wang, X. F.; Pang, W. Q. *J. Solid State Chem.* **2005**, *178*, 1003. (e) Dan, M.; Behera, J. N.; Rao, C. N. R. *J. Mater. Chem.* **2004**, *14*, 1257. (f) Norquist, A. J.; Thomas, P. M.; Doran, M. B.; O'Hare, D. *Chem. Mater.* **2002**, *14*, 5179. (g) Doran, M. B.; Norquist, A. J.; O'Hare, D. *Chem. Commun.* **2002**, 2946. (h) Fu, Y. L.; Ren, J. L.; Xu, Z. W.; Ng, S. W. *Acta Crystallogr.* **2005**, *E61*, m2738.

(13) (a) Fu, Y. L.; Xu, Z. W.; Ren, J. L. Ng, S. W. *Acta Crystallogr.* **2005**, *E61*, m1831. (b) Fu, Y. L.; Xu, Z. W.; Ren, J. L. Ng, S. W. *Acta Crystallogr.* **2005**, *E61*, m1641. (c) Fu, Y. L.; Xu, Z. W.; Ren, J. L. Ng, S. W. *Acta Crystallogr.* **2005**, *E61*, m593. (d) Fu, Y. L.; Xu, Z. W.; Ren, J. L. Ng, S. W. *Acta Crystallogr.* **2005**, *E61*, m1478.

(14) (a) Selbin, J.; Holmes, L. H.; McGlynn, S. P. *J. Inorg. Nucl. Chem.* **1963**, *25*, 1359. (b) Nakamoto, K. *Infrared and Raman Spectra of Inorganic and Coordination Compounds*; Wiley: NewYork, 1978.

Table 2. Crystal Data and Structure Refinement Parameters for **I-VI**

	I	**II**	**III**
empirical formula	$[C_2N_2H_{10}]_{1.5}[Fe(SO_4)_3]\cdot 2H_2O$	$[C_2N_2H_{10}][Fe(SO_4)_2(OH)]\cdot H_2O$	$[C_6N_2H_{18}]0.5[Fe(SO_4)_2(H_2O)_2]$
fw	473.2218	345.0991	341.10
shape	rod	rod	block
color	colorless	yellow	yellow
cryst syst	monoclinic	monoclinic	triclinic
space group	$P2_1/c$ (No. 14)	$P2_1/c$ (No. 14)	$P\bar{1}$ (No. 2)
a (Å)	9.0790(9)	6.9445(8)	5.6835(8)
b (Å)	20.3666(19)	10.2823(11)	9.1834(13)
c (Å)	8.8084(8)	15.1234(16)	10.3786(15)
α (deg)	90	90	86.839(3)
β (deg)	104.667(2)	90.932(2)	82.395(2)
γ (deg)	90	90	87.214(3)
V (Å^3)	1575.7(3)	1079.8(2)	535.65(13)
Z	4	4	2
ρ (g/cm^3)	1.995	2.123	2.105
μ (mm^{-1})	1.433	1.834	1.844
total data	15 849	4788	2797
unique data	3082	2113	1936
$R_{(int)}$	0.0769	0.0314	0.0171
R [$I>2\sigma(I)$]	R1 = 0.0573, wR2 = 0.1056	R1 = 0.0336, wR2 = 0.0865	R1 = 0.0460, wR2 = 0.1249
	R1 = 0.0737[a], wR2 = 0.1118[b]	R1 = 0.0420[a], wR2=0.0910[b]	R1 = 0.0537[a], wR2 = 0.1390[b]

	IV	**V**	**VI**
empirical formula	$[C_4N_2H_{12}][Fe_2(SO_4)_3(OH)_2(H_2O)_2]\cdot H_2O$	$[C_6N_2H_{18}]_{0.5}[Fe_2(SO_4)_3(H_2O)_4(OH)]\cdot H_2O$	$[C_6N_4H_{22}]_{0.5}[Fe(SO_4)_2(OH)]\cdot 2H_2O$
fw	577.0781	566.0609	358.118
shape	block	block	pole
color	red	yellow	green
cryst syst	orthorhombic	Triclinic	Tetragonal
space group	$Pca2_1$ (No. 29)	$P\bar{1}$ (No. 2)	$I4_1cd$ (No. 110)
a (Å)	20.0048(13)	7.3719(5)	19.5273(14)
b (Å)	7.2039(5)	7.4456(6)	19.5273(14)
c (Å)	12.2673(8)	16.5448(12)	12.1908(12)
α (deg)	90	87.6590(10)	90
β (deg)	90	87.0440(10)	90
γ (deg)	90	77.2220(10)	90
V (Å^3)	1767.9(2)	884.04(11)	4648.5(7)
Z	4	2	16
ρ (g/cm^3)	2.157	2.127	2.024
μ (mm^{-1})	2.087	2.088	1.707
total data	8372	4478	12904
unique data	3142	3010	2493
$R_{(int)}$	0.0320	0.0175	0.0677
R [$I>2\sigma(I)$]	R1 = 0.0302, wR2 = 0.0612	R1 = 0.0301, wR2 = 0.0800	R1 = 0.0563, wR2 = 0.1270
	R1 = 0.0345[a], wR2 = 0.0631[b]	R1 = 0.0338[a], wR2 = 0.0822[b]	R1 = 0.0686, wR2 = 0.1338

[a] $R1 = \sum||F_o| - |F_c||/\sum|F_o|$. [b] $wR2 = \{\sum[w(F_o^2 - F_c^2)^2]/\sum[w(F_o^2)^2]\}^{1/2}$.

microscope and glued to thin glass fibers with cyanoacrylate adhesive. Single-crystal data were collected on a Bruker SMART 1000 CCD diffractometer (graphite-monochromated Mo Kα radiation, $\lambda = 0.71073$ Å ($T = 298$ K)). Absorption corrections, based on symmetry-equivalent reflections, were applied using SADABS. The structures were solved by direct methods using SHELXS-97. The direct methods solution readily revealed the heavy-atom position (Fe and S) and allowed us to locate the other non-hydrogen positions (O, C, and N) from the Fourier difference maps. The hydrogen atoms for the amine molecules in **I**, **II**, **IV**, and **V** were located from the difference Fourier maps and placed in the observed positions and refined isotropically. In **III** and **V**, the hydrogen atoms for the amine molecules were placed theoretically. Some of the hydrogen atoms for the amine molecules in **VI** were not placed at the last circle because of the disorder of amine molecules. The hydrogen atoms for coordinated and uncoordinated water molecules were located from the difference Fourier maps in **I**, **II**, and **V**. However, the hydrogen atoms for the coordinated water molecules in **III** and for the uncoordinated water molecules in **IV** and **VI** were not entirely found in the last circle. The last cycles of refinement included atomic positions for all the atoms, anisotropic thermal parameters for all non-hydrogen atoms, and isotropic thermal parameters for all the hydrogen atoms. Details of the final refinements are given in Table 2. The selected bond lengths and angles are given in the Supporting Information.

Results

Crystal Structure. In these linear structures, all the Fe atoms are octahedrally coordinated to six O atoms, and the S atom is presented as the SO_4 tetrahedron. The Fe−O bond distances are in the range of 1.969(3)−2.031(3) Å with an average of 1.995 Å. The *cis*-O−Fe−O bond angles are between 85.14(13) and 94.20(14)°, [(*cis*-O−Fe−O)$_{av}$ = 90°]. The values of the bond distances and angles indicate that Fe forms a near-perfect FeO_6 octahedron. As a common feature

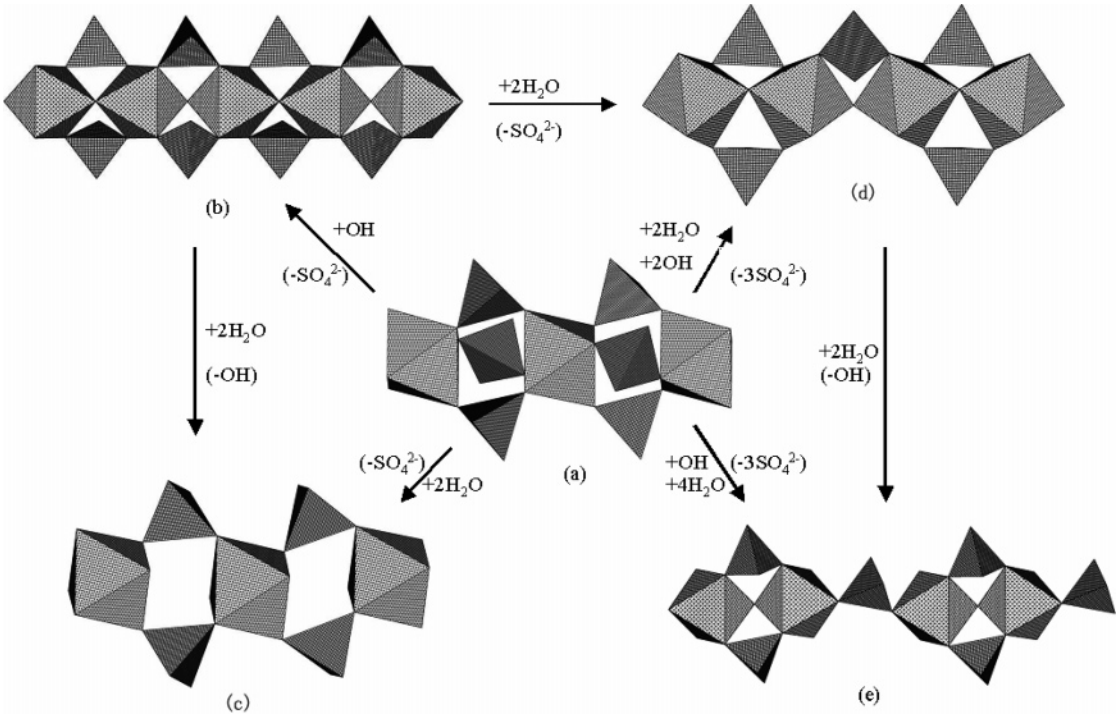

Figure 1. Structural correlation of the chains in **I**−**V** (octahedral FeO_6 and tetrahedral SO_4; a−e correspond to **I**−**V**).

among the six compounds, the SO_4 tetrahedron bridges two adjacent FeO_6 octahedra via a corner-sharing mode. The inorganic chain of **I** can be regarded as a parental motif and the others (**II**−**V**) are derived from structural replacement of the μ_2-SO_4 with μ_2-OH (or H_2O) groups. This interesting structural correlation among the inorganic chains in **I**−**V** is shown in Figure 1. In terms of the packing mode, some amine molecules are located around the inorganic chains; the others are located between the single-layers or double-layers built up from inorganic chains via interchain hydrogen-bonding interactions (Figure 2).

$[C_2N_2H_{10}]_{1.5}[Fe(SO_4)_3]\cdot 2H_2O$, I. The asymmetric unit of **I** contains 24 non-hydrogen atoms of which 16 belong to the inorganic framework with crystallographically distinct 1 iron atom and 3 sulfur atoms. Three SO_4 tetrahedra share corners with the adjacent FeO_6 octahedra resulting in a ferrinatrite-type[15] chain propagated along the *c* axis (Figure 1a). This linear topology can be found in iron[3d] and vanadium[3e] arsenates. The chains are surrounded by diprotonated ethylenediamine molecules and held together through N−H···O hydrogen bonding interactions to form a 3-D assembly (Figure 2a).

$[C_2N_2H_{10}][Fe(SO_4)_2(OH)]\cdot H_2O$, II. The asymmetric unit of **II** consists of 18 non-hydrogen atoms with crystallographically distinct 2 iron atoms and 2 sulfur atoms. The trans fashion of the μ_2-OH group creates a $\{-Fe-(OH)-Fe-\}_n$ backbone and allows the sulfate moiety as a symmetric bridge to form a tancoite-type[15] chain along the *a* axis (Figure 1b). The chain of **II** is similar to that of $[CN_3H_6]_2[FeF(SO_4)_2]$[8a] reported by Rao et al., the difference being that the F atom is substituted by OH groups. In addition to the synthetic materials, the analogous topology has also been observed in sulfate minerals.[16] The diprotonated ethylenediamine molecules around the chains hold the individual chains together into a 3-D assembly via N−H···O hydrogen-bonding interactions (Figure 2b).

$[C_6N_2H_{18}]_{0.5}[Fe(SO_4)_2(H_2O)_2]$, III. The asymmetric unit of **III** contains 16 non-hydrogen atoms of which 12 belong to the inorganic chain with crystallographically distinct 1 iron atom and 2 sulfur atoms. Along the *b* axis, two SO_4 tetrahedra share corners with adjacent FeO_6 octahedra resulting in an infinite 1-D chain containing four-membered rings (Figure 1c). The similar topology has also been observed in kröhnkite $Na_2[Cu(SO_4)_2(H_2O)_2]$.[17] These chains are arranged parallel to each other and held together by O−H···O hydrogen bonds to form a layerlike arrangement in the *ab* plane. The diprotonated TMED are located in the interlamellar space with the same orientation as the inorganic chains and hold such pseudolayers together via strong N−H···O hydrogen bonds (Table 3) to form a 3-D assembly (Figure 2c).

$[C_4N_2H_{12}][Fe_2(SO_4)_3(OH)_2(H_2O)_3]\cdot H_2O$, IV. The asymmetric unit of **IV** contains 28 non-hydrogen atoms of which 21 belong to the inorganic chain with crystallographically distinct 2 iron atoms and 3 sulfur atoms. The inorganic chain can be viewed as a derivative from the tancoite-type chain via partial replacement of μ_2-SO_4 groups by two water molecules (Figure 1d). In other words, it also can be viewed as a hybrid structure of tancoite and butlerite types. These chains are arranged parallel to each other and interact via O−H···O hydrogen bonds to form a layered arrangement in the *bc* plane (Figure 4). The pseudolayers are held together

(15) Hawthrone, F. C. *Tschermaks Mineral. Petrogr. Mitt.* **1983**, *31*, 121.

(16) (a) Mereiter, K. *Tschermaks Mineral. Petrogr. Mitt.* **1976**, *23*, 317. (b) Mereiter, K. *Acta Crystallogr.* **1990**, *C46*, 972.

(17) Hawthrone, F. C.; Krivovichev, S. V.; Burns, P. C. *Rev. Mineral. Geochem.* **2000**, *40*, 1.

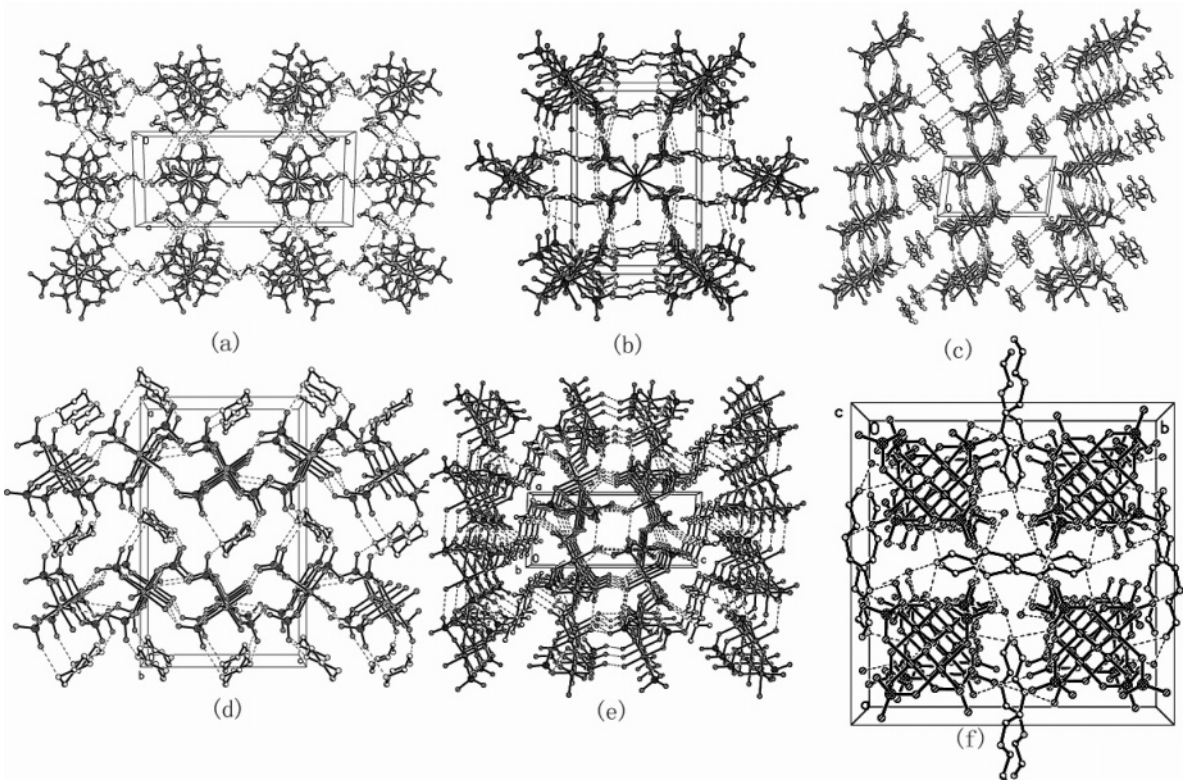

Figure 2. Perspective view of packing mode for the six compounds. The possible hydrogen bonds are represented by dotted lines: a−e correspond to **I**−**V**. The amine molecules are around the chains in a, b, and f and located between the layers in c, d, and e. For **VI**, the left- and right-handed chains are arranged alternatively.

through hydrogen-bonding interactions with the diprotonated piperazine molecules located in the interlamellar space to form a 3D assembly (Figure 2d).

$[C_6N_2H_{18}]_{0.5}[Fe_2(SO_4)_3(H_2O)_4(OH)]\cdot H_2O$, V. The asymmetric unit of **V** consists of 27 non-hydrogen atoms of which 22 belong to the inorganic chain with crystallographically distinct 2 iron atoms and 3 sulfur atoms. In the inorganic chains, the tancoite-type motifs in **II** are further connected by a tetrahedral SO_4 group via a corner-sharing mode, generating a new chain propagating along the *b* axis (Figure 1e). Such topology has also been observed in copiapite.[18] The neighboring chains interact with each other through O−H···O hydrogen bonds to generate a layerlike arrangement in the *ab* plane. It is more interesting that two neighboring pseudolayers are joined via O−H···O hydrogen-bonding interactions, leading to a double-layer (Figure 2e). The diprotonated TMEA with the same orientation as the inorganic chains is located between these double-layers and interacts with inorganic framework via N−H···O hydrogen bonds (Table 3).

$[C_6N_4H_{22}]_{0.5}[Fe(SO_4)_2(OH)]\cdot 2H_2O$, VI. The asymmetric unit of **VI** includes 19 non-hydrogen atoms of which 13 belong to the inorganic framework. The structural motif of **VI** is similar to that of **II**, but within the chain, the μ_2-OH group adopts a cis rather than trans fashion to form an interesting chiral chain (Figure 3). The left-handed and right-handed chains are arranged alternatively and held together via N−H···O hydrogen bonds with the amines and water molecules to generate a 3-D assembly (Figure 2f). The orientation of the linear TETA molecules is perpendicular to the helical chain. To the best of our knowledge, it is a rare example of a compound with helical chains among the metal sulfates.

Discussion

Synthesis. The results indicate that the reaction parameters greatly influenced the types of the products (Table 1). The ratio of H_2SO_4/amine in all cases was ≥ 1 to avoid the precipitation of Fe^{3+}. Because of the consistent ratio of diamine/H_2SO_4, the pH did not vary among the mentioned reactions. It is found that the ratio of Fe/S and the net amount of sulfuric acid in the starting mixture are responsible for the sulfated extent of the chains. In the $Fe_2(SO_4)_3/H_2SO_4$/en system, the ratio of 1.0:4.5:8.0 with a lower concentration of Fe^{3+} and a higher concentration of H_2SO_4 led to a colorless crystal product (**I**). However, the ratio of 1.0:1.0:1.0 with a higher concentration of Fe^{3+} and a lower concentration of H_2SO_4 resulted in a yellow crystal product (**II**). In the piperazine system, a higher concentration of Fe^{3+} led to a new phase, **IV**, as the second product during the preparation of a known compound, $[C_4H_{10}N_2][Fe(SO_4)_2(OH)]$.[12] Similar modulation of other amine systems did not lead to new products.

Furthermore, the type of amines is another factor in obtaining chains with various sulfated extents. First, the results indicate that 1,2-substitued diamine is advantageous for obtaining crystalline products, such as en, piperazine, and

(18) (a) Fanfani, L.; Nunzi, A.; Zanazzi, P. F.; Zanzari, A. R. *Am. Mineral.* **1973**, *58*, 314. (b) Suesse, P. *Neues Jahrb. Mineral., Monatsh.* **1970**, 286.

Table 3. Hydrogen Bonds for Compounds **I**−**VI** (Å)[a]

D−H···A	*d*(D···A)	D−H···A	*d*(D···A)
		I	
N(1)−H(1)···O(13)	2.767(7)	O(14)−H(11)···O(10)#8	2.812(6)
N(1)−H(1)···O(9)#2	2.874(5)	O(14)−H(12)···O(9)#9	2.854(7)
N(1)−H(2)···O(4)	3.003(6)	N(3)−H(16)···O(12)#7	2.836(6)
N(1)−H(2)···O(12)	3.128(6)	N(3)−H(17)···O(9)#2	2.843(6)
N(1)−H(3)···O(7)#4	2.812(6)	N(3)−H(15)···O(10)#2	2.810(6)
N(1)−H(3)···O(8)	3.141(6)	N(3)−H(15)···O(3)	3.334(6)
N(2)−H(9)···O(7)#5	2.848(6)	N(2)−H(8)···O(8)	2.949(6)
N(2)−H(9)···O(8)#1	3.025(6)	N(2)−H(8)···O(7)#4	3.056(6)
O(13)−H(14)···O(14)#6	2.772(8)	N(2)−H(10)···O(11)#5	2.940(6)
O(13)−H(13)···O(11)#7	2.748(6)		
		II	
N(1)−H(1)···O(9)#8	3.003(4)	O(3)−H(13)···O(10)	2.697(5)
O(10)−H(12)···O(9)#3	3.142(4)	N(2)−H(8)···O(8)#1	2.739(4)
O(10)−H(12)···O(8)#3	3.134(5)	N(2)−H(10)···O(1)#11	2.894(4)
N(1)−H(2)···O(6)#1	2.745(4)	N(2)−H(9)···O(4)#11	3.200(3)
N(1)−H(3)···O(7)#7	2.943(4)	N(2)−H(9)···O(5)#11	2.982(4)
O(10)−H(11)···O(6)#10	2.898(4)		
		III	
N(1)−H(5)···O(9)#12	2.795(5)	O(2)−H(2)···O(7)#5	2.940(4)
O(4)−H(4)···O(8)#13	2.721(4)	O(2)−H(2)···O(8)#20	2.984(5)
O(2)−H(2)···O(8)	3.203(5)		
		IV	
O(1)−H(5)···O(12)#14	2.613(5)	N(2)−H(2D)···O(13)#16	2.737(5)
O(4)−H(4)···O(15)#15	2.922(5)	N(2)−H(2C)···O(8)#12	3.253(5)
O(16)−H(3)···O(15)	2.735(5)	N(2)−H(2C)···O(11)#12	2.847(5)
O(16)−H(2)···O(9)#14	3.092(5)	N(1)−H(1C)···O(14)#16	2.860(5)
O(16)−H(2)···O(3)#14	2.725(5)	N(1)−H(1D)···O(17)	2.757(5)
O(2)−H(1)···O(3)#14	2.724(4)	O(2)−H(6)···O(15)#13	2.757(5)
		V	
O(18)−H(20)···O(12)	3.139(3)	O(10)−H(9)···O(14)#18	3.011(3)
O(18)−H(20)···O(7)	3.087(4)	O(15)−H(8)···O(8)#19	2.731(3)
N(1)−H(15)···O(16)#17	2.767(4)	O(15)−H(7)···O(6)#13	2.669(3)
O(18)−H(13)···O(8)#7	2.740(4)	O(13)−H(6)···O(17)#18	2.659(3)
O(11)−H(12)···O(18)#7	2.713(4)	O(13)−H(5)···O(1)#13	2.712(3)
O(11)−H(11)···O(6)#18	2.720(3)	O(9)−H(1)···O(18)#13	2.774(3)
O(10)−H(10)···O(1)#18	2.864(3)		
		VI	
N(2)−H(2B)···O(9)#21	3.09(2)	N(1)−H(1A)···O(8)#24	3.004(19)
N(2)−H(2C)···O(3)#22	2.99(2)	N(1)−H(1C)···O(10)#25	2.94(2)
N(1)−H(1A)···O(1)#23	2.837(18)	O(4)−H(1)···O(8)	3.109(17)

[a] Symmetry transformations used to generate equivalent atoms: #1 x, $-y+3/2$, $z+1/2$; #2 x, $-y+3/2$, $z-1/2$; #3 $-x+1$, $y+1/2$, $-z+1/2$; #4 $x-1$, $-y+3/2$, $z-1/2$; #5 $x-1$, y, z; #6 x, y, $z-1$; #7 $-x+1$, $-y+1$, $-z+1$; #8 $-x+2$, $-y+1$, $-z+1$; #9 $-x$, $y-1/2$, $-z+3/2$; #10 $-x+1$, $y-1/2$, $-z+1/2$; #11 $-x+1$, $-y+2$, $-z+1$; #12 x, y, $z+1$; #13 $x+1$, y, z; #14 $-x+3/2$, y, $z+1/2$; #15 $-x+3/2$, $y-1$, $z-1/2$; #16 $x+1/2$, $-y+1$, z; #17 $x-1$, $y+1$, z; #18 x, $y+1$, z; #19 $-x+2$, $-y$, $-z+1$; #20 $-x+1$, $-y$, $-z+1$; #21 $-y+1/2$, $x+1$, $z+3/4$; #22 x, $-y+1$, $z+1/2$; #23 x, $y+1$, $z+1$; #24 $-x+1/2$, $y+1/2$, $z+1$; #25 $-y+1/2$, $-x+1$, $z+1/4$.

diethylenetriamine.[13] Under the same experimental conditions, 1,3-diaminopropane and 1,4-diaminobutane have also been introduced, and no crystal was obtained, possibly because of their size, although 1,6-hexanediamine[20] leads to the same inorganic motif as **II**, probably because of its main charge-compensated effect only as dications. Second, the diamines with different substituted extents also direct the reaction toward various structures with different sulfated extents, such as TMED. Third, when TETA was introduced as a directing agent, the novel helical chain of **VI** was separated as an exceptional situation.

Hydrolysis is of importance for the aqueous chemistry of the Fe^{3+} ion.[1,19] Interestingly, a reddish brown gel was always observed in the starting mixtures before hydrothermal treatment, implying existence of highly polymerized oxo-iron clusters.[21] It is also suggested that the high-hydrolytic polymer can be separated through incorporating appropriate directing agents. The synthesis of an isolated tetranuclear iron sulfate cluster incorporating 4,4′-bipyridine may exemplify this presumption.[22]

Structural Discussion. As mentioned above, the tancoite-type $[Fe(SO_4)_2(OH)]$ unit as a common building block in **II**, **IV**, **V**, and **VI** and can be formulated as $[M(TO_4)_2L]$ (T = 4-coordinated cation, L = unspecified anion ligand) which is also described in synthetic vanadium sulfate,[11] fluoride iron-sulfates, [7] and Al,[23] Ga,[24] and Fe[25] phosphates including their minerals.[14,15,26] On the basis of this unit and amines, these inorganic 1-D chains exhibit diverse topologies with structural correlations, although they cannot be transformed experimentally.

It is noteworthy that the sulfated extent of the chain decreases gradually with the increase of substituted extent of the amino group (primary, secondary, and tertiary amine): namely, the fewer hydrogen atoms bind to the amino group, the fewer hydrogen bonds are formed between the amines and the inorganic chains. The chains with a low sulfated extent can be observed in **III** and **V** incorporating TMED, as well as in **IV** incorporating piperazine. Such chains were decorated by hydroxyl groups and coordinated water molecules via hydrolysis and hydration to generate distinct topologies. The amines can be related to the charge balancers and hydrogen-bond donors because of the precedence of the chains in **III** and **V** in mineral kröhnkite and copiapite, respectively.

In terms of the packing characteristics, the chains with different compositions always exhibit distinct stacking manners involving N−H···O and O−H···O hydrogen-bonding interactions. The inorganic chains with high sulfated extents tend to interact with diprotonated amines, leading to the individual chains being surrounded by amines in **I** and **II** (Figure 2). The inorganic chains with low sulfated extents are inclined to interact with each other to form layered arrangements in **III**, **IV**, and **V** (Figure 2). It is suggested that the ability of OH^- and H_2O ligands to donate hydrogen

(19) Lii, K. H.; Huang, Y. F.; Zima, V.; Huang, C. Y.; Lin, H. M.; Jiang, Y. C.; Liao, F. L.; Wang, S. L. *Chem. Mater.* **1998**, *10*, 2599.
(20) Fu, Y. L.; Xu, Z. W.; Ren, J. L. Ng, S. W. *Acta Crystallogr.* **2005**, *E61*, m596.
(21) Flynn, C. M. J. *Chem. Rev.* **1984**, *84*, 31.
(22) Fu, Y. L.; Xu, Z. W.; Ren, J. L. Unpublished work.
(23) (a) Attfield, M. P.; Morris, R. E.; Burshtin, I.; Campana, C. F.; Cheetham, A. K. *J. Solid State Chem.* **1995**, *118*, 412. (b) Lii, K. H.; Wang, S. L. *J. Solid State Chem.* **1997**, *128*, 21.
(24) (a) Walton, R. I.; Millange, F.; Bail, A. L.; Loiseau, T.; Serre, C.; O'Hare, D.; Ferey, G. *Chem. Commun.* **2000**, 203. (b)Lin, H. M.; Lii, K. H. *Inorg. Chem.* **1998**, *37*, 4220. (c)Walton, R. I.; Millange, F.; O'Hare, D.; Paulet, C.; Lossieau, T.; Férey, G. *Chem. Mater.* **2000**, *12*, 1979. (d) Bonhomme, F.; Thoma, S. G.; Nenoff, T. M. *J. Mater. Chem.* **2001**, *11*, 2559.
(25) (a) Cavellec, M.; Riou, D.; Férey, G. *Inorg. Chem. Acta.* **1999**, *291*, 317. (b) Cavellec, M.; Riou, D.; Greneche, J. M.; Férey, G. *Inorg. Chem.* **1997**, *36*, 2187. (c) Choudhury, A.; Rao, C. N. R. *Zh. Struct. Khim.* **2002**, *43*, 681. (d) Mahesh, S.; Green, M. A.; Natarajan, S. *J. Solid State Chem.* **2002**, *165*, 334. (e) Lii, K. H.; Huang, Y. F. *Chem. Commun.* **1997**, 1311. (f) Moore, P. B.; Araki, T. *Am. Mineral.* **1974**, *59*, 964. (g) Moore, P. B.; Araki, T. *Am. Mineral.* **1977**, *62*, 692.
(26) Hawthorne, F. *Acta Crystallogr.* **1994**, *B50*, 481.

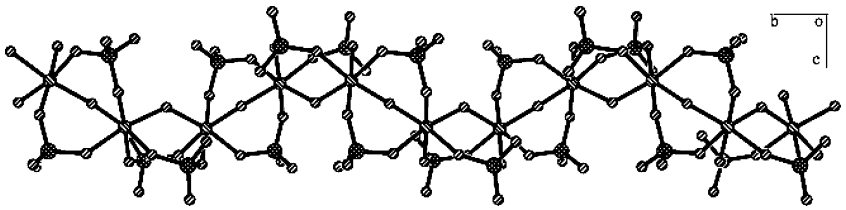

Figure 3. Stick and ball view of the helical chains of **VI** along the *b* axis.

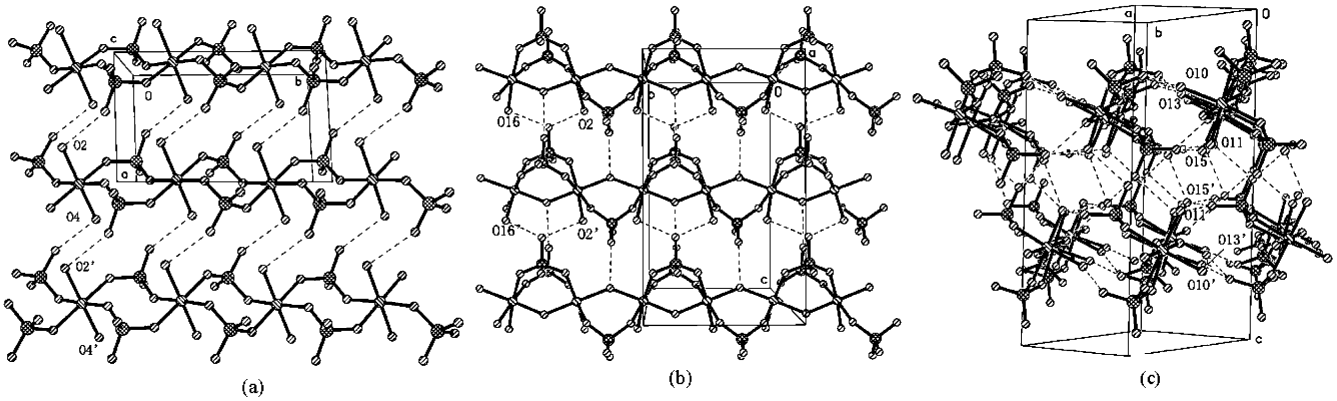

Figure 4. Hydrogen-bond scheme of the pseudolayers for **III** (a), **IV** (b), and **V** (c). The complex hydrogen-bond network involving cis vertex-coordinated water molecule to form double-layers in c. (The oxygen atoms of coordinated water molecules are labeled, and all hydrogen atoms are omitted for clarity.)

bonds is the main factor, while the amines probably have very little influence. (Table 3, Figure 4). Moreover, the amount and position of coordinated waters affect the arrangement fashion. For **IV**, one water molecule coordinates to each Fe atom, and the inorganic chains are held together to form a single-layer arrangement (Figure 4b). In contrast to **IV**, both **III** and **V** have two water molecules coordinated to each Fe atom in trans and cis configurations, respectively. Interestingly, the inorganic chains in **III** are held together to form a single-layer arrangement, while those in **V** are held together to form a double-layer arrangement (Figure 4). One can find that the coordinated water molecules in the cis configuration not only result in the single-layers but also bring them together to form double-layers. The hydrogen-bonding interactions between amines and such pseudolayers stabilize the 3D assembly (Table 3).

The featured arrangements for the amine molecules involve their orientations. The en, piperazine,[13] and 1,6-hexanediamine[20] molecules are perpendicular to the same inorganic chain, as in **II**. Moreover, the linear topology of **II** has been observed in its sodium salt minerals;[17] hence, the charge-compensated effects of such amines may be the dominant factors. In addition, compared with the orientation of the diamines in widely reported metal phosphates, the piperazine molecules in **IV** and the TMED molecules in **III** and **V** adopt the same orientation and are parallel to the inorganic chains.

To the best of our knowledge,[7] **III**, **IV**, and **VI** belong to the new topology geometries in iron sulfate. **III** represents an octahedral−tetrahedral (O−T) chain that can be considered as a rare perfect kröhnkite-type[15] topology in the iron sulfate family. For building higher-dimensional structures, the synthesis of the corner-shared chains, like **III**, is rather significant.[28] The chain of **IV** is much like a hybrid pattern of tancoite- and butlerite-type chains, although they have been synthesized in different systems,[8a] respectively. Here, one can find that the different mineral characteristics can be displayed in one structure. When viewed as a result of the transformation of the trans linkage of **II** to the cis linkage, **VI** exhibits interesting helical chains with a 4_1 screw axis incorporating achiral amines. The design and synthesis of inorganic materials with helical structures are of particular interest and are a great challenge.[29] The reason for the generation of chirality is not well understood, and the relevant study is ongoing.

Conclusion

Organically directed iron sulfates were synthesized under hydrothermal conditions. The ratio of reactants in the starting mixtures, the types of amines, and especially, the hydrogen-bonding interactions are three crucial factors for the construction of inorganic frameworks and their packing modes. The study will be an aid in the understanding of the directing mechanism of amines for the construction of more complex structures.

Acknowledgment. We thank the Natural Scientific Foundation Committee of Shanxi Province (20041031) for generously supporting this study.

Supporting Information Available: IR spectra, powder XRD patterns, TGA curves of **I**−**VI**, hydrogen-bonding interactions in **I**−**VI**, and crystallographic data for **I**−**VI** (CIFs). This material is available free of charge via the Internet at http://pubs.acs.org.

IC061059V

(27) Rao, C. N. R.; Nagarajan, S.; Choudhury, A.; Neeraj, S.; Ayi, A. A. *Acc. Chem. Res.* **2001**, *34*, 80−87.
(28) Choudhury, A.; Neeraj, S.; Natarajan, S.; Rao, C. N. R. *J. Mater. Chem.* **200**1, *11*, 1537.
(29) Xiao, D. R.; Hou, Y.; Wang, E. B.; An, H. Y.; Lu, J.; Li, Y. G.; Xu, L.; Hu, C. W. *J. Solid State Chem.* **2004**, *177*, 2699−2704.